CHEMISTRY
A EUROPEAN JOURNAL

DOI: 10.1002/chem.201200362

Controllable Self-Assembly of Organic–Inorganic Amphiphiles Containing Dawson Polyoxometalate Clusters

Panchao Yin,[a] Chullikkattil P. Pradeep,[b] Baofang Zhang,[a] Feng-Yan Li,[b] Claire Lydon,[b] Mali H. Rosnes,[b] Dong Li,[a] Emily Bitterlich,[a] Lin Xu,[c] Leroy Cronin,*[b] and Tianbo Liu*[a]

Abstract: An organic–inorganic molecular hybrid containing the Dawson polyoxometalate, $((C_4H_9)_4N)_5H[P_2V_3W_{15}O_{59}(OCH_2)_3CNHCOC_{15}H_{31}]$, was synthesized and its surfactant-like amphiphilic properties, represented by the formation of bilayer vesicles, were studied in polar solvents. The vesicle size decreases with both decreasing hybrid concentration and with increasing polarity of the solvent, independently. The self-assembly behavior of this hybrid can be controlled by introducing different counterions into the acetonitrile solutions. The addition of $ZnCl_2$ and NaI can cause a gradual decrease and increase of vesicular sizes, respectively. Tetraalkylammonium bromide is found to disassemble the vesicle assemblies. Moreover, the original counterions of the hybrid can be replaced with protons, resulting in pH-dependent formation of vesicles in aqueous solutions. The hybrid surfactant can further form micro-needle structures in aqueous solutions upon addition of Ca^{2+} ions.

Keywords: organic–inorganic hybrid composites · polyoxometalates · self-assembly · surfactants · vesicles

Introduction

Polyoxometalates (POMs) are a large group of anionic metal oxide clusters with varied topologies, sizes, and charge densities, composed of early-transition-metal ions in high oxidation states and oxo ligands.[1] POMs have been widely studied for their applications in the development of magnetic and photo-electronic materials, catalysts, and medicines.[1–2] POMs are also used in industry as catalysts and electrode materials.[3] In recent years, the self-assembly behavior of POMs has received continuous interest, because it helps to incorporate POMs into nano-devices with desired morphology and functionality, which consequently expands the applicability of POMs.[4]

Various methods are available to assemble POMs into nano- and micro-structures. As a well-developed protocol, supramolecular interaction-driven self-assembly, including coordination and hydrogen bonding, has been used to obtain oligomers of POMs,[5] POM-based nanocages,[6] nanorods,[7] and 3D-frameworks.[8] Due to the macroionic feature of POM anions, counterion-mediated self-assembly leads to the formation of hollow, spherical "blackberry" structures in solutions as well as monolayers of close-packed POM clusters on surfaces.[4a–c,9] Self-assembly of POMs based on solvophobic interactions has also been achieved by using surfactant-encapsulated POMs[10] and/or POM–organic hybrids.[11] In the latter approach, several types of POM hybrids with different molecular architectures (dumbbells, POMs functionalized with single or double alkyl chains, etc.) have been successfully explored for their amphiphilic properties in solution and at interfaces.[11–12] Therefore, these POM-based hybrids can be considered as unique types of surfactants with bulky polar head groups.

So far, hybrids containing several types of POM clusters have been explored. Anderson-type POMs functionalized with two long alkyl chains were found to form bilayer vesicle structures in acetonitrile/water mixed solvents, and reverse vesicle structures in acetonitrile/toluene mixed solvents.[13] The vesicle size can be tuned by solvent composition. Moreover, the vesicles of a Lindqvist hexavanadate-based hybrid surfactant were found to demonstrate interesting fluorescence properties associated with the self-assembly process.[12] The surfactants with Keggin-type POM as polar head groups were found by Polarz et al. to be able to self-as-

[a] P. Yin, B. Zhang, D. Li, E. Bitterlich, Prof. Dr. T. Liu
Department of Chemistry
Lehigh University
Bethlehem, PA 18015 (USA)
Fax: (+1) 6107586536
E-mail: liu@lehigh.edu

[b] Dr. C. P. Pradeep, Dr. F.-Y. Li, C. Lydon, Dr. M. H. Rosnes, Prof. Dr. L. Cronin
WestCHEM, School of Chemistry
University of Glasgow
University Avenue, Glasgow, G12 8QQ (UK)
Fax: (+44) 1413304888
E-mail: lee.cronin@glasgow.ac.uk

[c] Prof. Dr. L. Xu
Key Laboratory of Polyoxometalate Science
of the Ministry of Education, Department of Chemistry
Northeast Normal University
Changchun, Jilin (P.R. China)

Supporting information for this article is available on the WWW under http://dx.doi.org/10.1002/chem.201200362.

 © 2012 Wiley-VCH Verlag GmbH & Co. KGaA, Weinheim

semble into micelles and lyotropic phases.[11] The surfactants were later observed to self-assemble into a hexagonal lattice at the air/water interface.[11b] However, the research in this area has only just started and is still far from achieving the aim of rationally controlling the self-assembly process of hybrids by designing their architectures to facilitate their applications. One important POM-type lacking detailed studies as a polar head group in single-cluster hybrid surfactants is the Dawson cluster. Earlier studies on single Dawson-based hybrids were carried out mainly on bulk samples and/or at interfaces, leaving their detailed solution behavior unexplored.[14] Herein, we report the synthesis of a single Dawson-cluster-based organic–inorganic hybrid and its concentration-, polarity-, counterion-, and pH-dependent self-assembly behaviors in solution, determined by using laser light scattering (LLS), electron microscopy, and ^{1}H NMR techniques.

Results and Discussion

Due to the existence of symmetrical functional positions on the surfaces of Anderson, Lindqvist and Keggin clusters, the hybrid surfactants containing such polar head groups usually have two alkyl tails.[11–13] However, the two caps of the substituted Dawson cluster, $[P_2V_3W_{15}O_{62}]^{9-}$, are asymmetrical, with the vanadate cap comparatively more reactive than the tungstate one. Therefore, it is possible to synthesize single-tailed hybrids based on this cluster. Similar to the synthesis of Dawson-based dumbbell molecules,[15] the organic ligand L^1 with a 15-carbon alkyl chain and tris(hydroxymethyl)amidomethane moiety was initially synthesized and then reacted with $[P_2V_3W_{15}O_{62}]^{9-}$ obtaining the target molecule $((C_4H_9)_4N)_5H[P_2V_3W_{15}O_{59}(OCH_2)_3CNHCOC_{15}H_{31}]$ (TBA·Ds; TBA = $((C_4H_9)_4N)^+$; Ds = surfactant anion), molecular structure of which was confirmed by ^{1}H NMR, IR spectroscopies, and elemental analysis (see the Supporting Information, the Experimental Section, and Figure 1). The original counterions, five TBA molecules, can be replaced with protons by passing an acetonitrile solution of TBA·Ds through a column filled with a cation-exchange resin (see the Supporting Information). The resulting new compound $H_6[P_2V_3W_{15}O_{59}(OCH_2)_3CNHCOC_{15}H_{31}]$, H·Ds, is soluble in both acetonitrile and water.

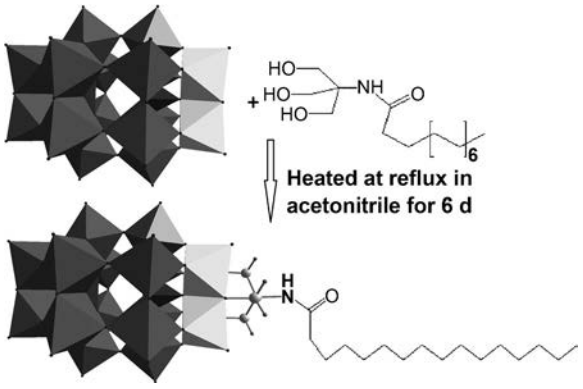

Figure 1. The synthesis of the surfactant with Dawson-type POMs as polar head group. Polyhedron color code: W = grey; P = black; V = white.

Critical association concentration (CAC): The acetone solutions of TBA·Ds with concentrations ranging from 0.002 to 0.5 mg mL^{-1} were prepared and monitored by static-light scattering (SLS) at 90° scattering angle. It was expected that the scattered intensity would increase significantly, if large self-assembled aggregates were formed in the solutions. Correspondingly, a sudden, drastic increase in the equilibrium-scattered intensity at a given TBA·Ds concentration would indicate the attainment of the critical association concentration (CAC), which was found to be 0.02 mg mL^{-1} in the present case. The solutions with concentrations below the CAC showed very low scattered intensities (< 400 kcps; scattered intensity for benzene is 120 kcps), indicating the absence of large assemblies (Figure 2a). Dynamic-light scattering (DLS) and SLS were applied to determine the hydrodynamic radius (R_h) and radius of gyration (R_g) of the assemblies formed at different concentrations (Figure 2c and Figure S1 in the Supporting Information). R_h values of the assemblies showed narrow distributions and no angular dependence, suggesting spherical structure for the assemblies. The ratio of R_h/R_g is close to 1, indicating a hollow spherical structure. The vesicular structure and the sizes of the assemblies were confirmed by TEM studies (Figure 2d). Interestingly, contrary to the hexavanadate-based hybrids ($TBA_2[V_6O_{13}\{(OCH_2)_3CCH_2OOC(CH_2)_{16}CH_3\}_2]$ ($\{V_6\}$), see the Supporting Information), self-assembly behavior and assembly sizes of which are concentration independent,[12] the vesicle size observed here increases from 50 to 115 nm, as the

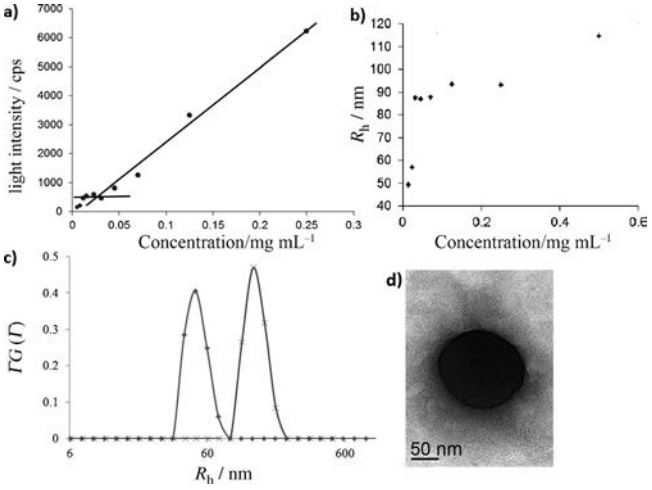

Figure 2. a) Scattered intensities at 90° scattering angle of the TBA·Ds in acetone at different concentrations. b) Hydrodynamic radius of the formed vesicle structures in the TBA·Ds acetone solution depending on the concentration. c) DLS results of 0.5 (×) and 0.03 (◆) mg mL^{-1} TBA·Ds acetone solution at 30° scattering angle. d) TEM images of the vesicle structure from the 0.5 mg mL^{-1} TBA·Ds in acetone solution.

 © 2012 Wiley-VCH Verlag GmbH & Co. KGaA, Weinheim

concentration is raised from 0.02 to 0.5 mg mL^{-1} (Figure 2b).

Effect of solvent polarity: For solutions with a given POM-hybrid concentration, the vesicle size can be tuned by adjusting the solvent polarity. Solutions of 0.02 mg mL^{-1} TBA·Ds in pure acetone, pure acetonitrile, and acetone/water mixed solvents containing 95:5, 85:15, 65:35, and 50:50 vol% of acetone:water, respectively, were prepared. The vesicle sizes measured by DLS and TEM (Figure 3)

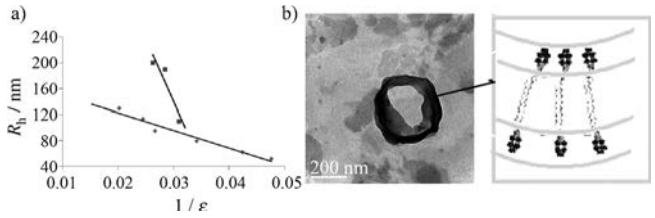

Figure 3. a) The plot of the hydrodynamic radius of vesicles versus the inverse of the dielectric constant of the solvent. Data of Dawson-based surfactant are represented by ◆, whereas ■ represents that of hexavanadate-based surfactant (V_6 surfactant). b) TEM images of the vesicle structure formed by TBA·Ds in the mixture of water/acetone (1:1) with a proposed model for the bilayer structure.

showed a linear relationship with the inverse of the dielectric constant of the solvent, indicating a charge-regulated process.[4a] The solvent-polarity dependent self-assembly can be explained by the dissociation of the TBA counterions from the POM surface, consequently increasing the hydrophilicity of the polar head groups. The counterion dissociation can clearly be observed by comparing the diffusion coefficients of counterions and the anionic hybrids in acetone and acetonitrile solutions by diffusion-ordered spectroscopy (DOSY) NMR technique. In polar solvents (acetonitrile), the TBA counterions diffuse much faster than the hybrid cluster, which leads to the TBA disassociation; however, the two parties showed very close diffusion speed in the relatively nonpolar solvent acetone, (Figure 4) indicating strong TBA association around the POM.

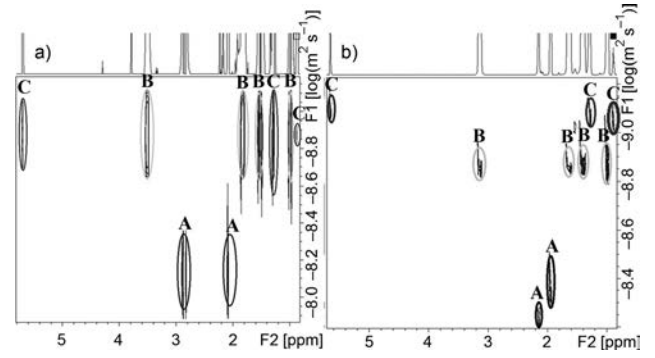

Figure 4. DOSY–NMR results of TBA·Ds in a) acetone and b) acetonitrile. A circle = solvent; B circle = tetrabutylammonium; C circle = surfactant anion.

The vesicle size of $\{V_6\}$ surfactant showed similar dependence on the solvent polarity, but with a much more negative slope than that of TBA·Ds (Figure 3a), which could be related to the less negative charge of $\{V_6\}$ (−2) compared with the TBA·Ds (−6).[12] The counterion disassociation is controlled by factors, such as static charge interaction, solvent polarity, and solvation of ions. Static-charge force is proportional to the number of charges of the ions and thus, TBA could be easier to diffuse away from the surface of the $\{V_6\}$ polar head groups of the surfactant than from Dawson clusters (TBA·Ds**)**. Therefore, the effective charge on the $\{V_6\}$ surfactant increases more significantly when the solvent polarity increases, which finally results in a more negative slope in Figure 3a. For the $\{V_6\}$ surfactant, vesicles could only be observed when 20–35 vol% of water was added to its acetone solution.[12] However, due to the high negative charge (−6) and much larger polar head group, TBA·Ds can form vesicle structures in less polar solvents, such as pure acetone.

Effect of counterions: Counterions play a critical role in colloid systems and biological systems, such as the folding of RNA molecules,[16] the formation of virus capsid structures,[17] and in the stabilization of biological macromolecules.[18] Due to their high charge density and hydrophilic nature, POMs exhibit strong counterion-dependent self-assembly, catalytic behavior, and stability.[4c] In particular, counterion distribution around hydrophilic macroanions and selective monovalent cation association and exchange around Keplerate POM macroanions in dilute aqueous solutions are unique and directly related to their self-assembly process.[19] On the other hand, counterions can also affect the behavior of common surfactants in aqueous solution at air/solution interfaces or at solid/solution interfaces and in the micelle-to-vesicle transition processes.[20] Therefore, the effect of counterions on the self-assembly of POM-containing hybrids is an interesting avenue, worth further investigation.

TBA·Ds is not soluble in water, but soluble in polar organic solvents, such as acetone and acetonitrile. Different salts, $ZnCl_2$, $CuCl_2$, NaI, tetrabutylammonium iodide (TBA·I), and dodecyltrimethylammonium bromide (DTMA·Br), which are soluble in acetonitrile, were added to acetonitrile solutions of TBA·Ds, respectively, to study the role of the counterions on the vesicle formation and vesicular sizes. The vesicle size decreased gradually with increasing concentration of $ZnCl_2$. Interestingly, the vesicle size remains unchanged at first upon addition of NaI, but gradually increases when the NaI concentration exceeds 0.03 mg mL^{-1} (Figure 5a). DOSY measurements indicated that the addition of NaI increased the diffusion coefficient (D) of TBA cations (without NaI, $D = 1.386 \times 10^{-9}$ m^{2}s^{-1}; with 0.1 mg mL^{-1} NaI, $D = 2.019 \times 10^{-9}$ m^{2}s^{-1}), suggesting that the additional counterions replace the original TBA counterions around the Dawson clusters and subsequently release TBA cations into the solution. $ZnCl_2$, which is quite solvated in acetonitrile, prefers coordinating to the terminal

 © 2012 Wiley-VCH Verlag GmbH & Co. KGaA, Weinheim

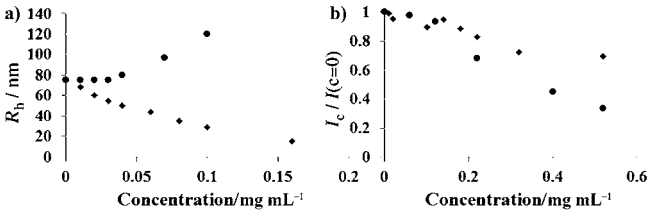

Figure 5. a) The plot of hydrodynamic radius versus the concentration of added salt. Circle = NaI; square = $ZnCl_2$. b) The plot of the reduced scattered intensity at 90° scattering angle versus the concentration of added salt. ● = TBA·I; ◆ = TMDA·Br.

or bridging oxo ligands on the surface of the Dawson clusters, forcing the polar domains to be exposed to the solvent environment, which in turn increases the curvature of the vesicle, that is, the vesicle size becomes smaller. Upon the addition of NaI, on the other hand, the sodium ions contribute to shielding the high negative charges of the polar head groups from each other, and thus reduce the repulsion between the polar heads on the surface of the vesicle. The curvature of the vesicle decreases, and as a result, the vesicle size increases. The same argument can be used to explain the formation of larger vesicles from H·Ds (R_h = 110 nm), compared with vesicles obtained from TBA·Ds (R_h = 75 nm), both in acetonitrile.

The additions of $CuCl_2$, TBA·I, or DTMA·Br show no obvious effect on the vesicle size as those cations are not able to replace the TBA cations that surround the polar Dawson clusters. However, TBA·I and DTMA·Br were observed to cause the disassembly of the vesicles, and this is confirmed by the fact that the scattered intensities from corresponding solutions drop increasingly, when more of these salts were added (Figure 5b). Further, addition of TBA·I and DTMA·Br does not liberate the original TBA counterions, but results in a gradual accumulation of the hydrophobic cations around the hydrophilic Dawson clusters, causing a decrease in the hybrid molecule's amphiphilic nature. The TBA counterions dissociate the vesicle structures faster than DTMA, possibly due to the comparatively smaller volume of the TBA cations, which allows a larger amount of TBA cations to move closer to the POM, compared with the larger DTMA cations.

Effect of pH: pH-sensitive vesicle structures are important for applications in sensing, imaging, and drug-delivery systems.[21] $\{Mo_{72}Fe_{30}\}$, a POM macromolecule, showed pH-controlled deprotonation in aqueous environment (like a weak acid) and resulted in pH-dependent assembled "blackberry" sizes.[22] H·Ds is water soluble, and its Dawson cluster polar-head group behaves like a nanoacid, negative charges of which can be tuned by changing the pH of the solution.

The pH of the 1.0 mg mL^{-1} aqueous solution of H·Ds is 2.99, corresponding to the release of approximately four protons per Dawson cluster. Vesicle structures with R_h of about 67 nm were observed from this solution by light-scattering experiments. Interestingly, the R_h of the vesicle structures gradually decreased to 64 nm at pH 5, whereas the R_h increased to 81 nm at pH 1.5. A plateau area appeared from pH 5 to 9 with R_h of about 64 nm. However, R_h value decreased sharply to 38 nm, when pH was changed from 9 to 12 (Figure 6b). Further experiments indicated that the pH-dependent self-assembly process can be done reversibly.

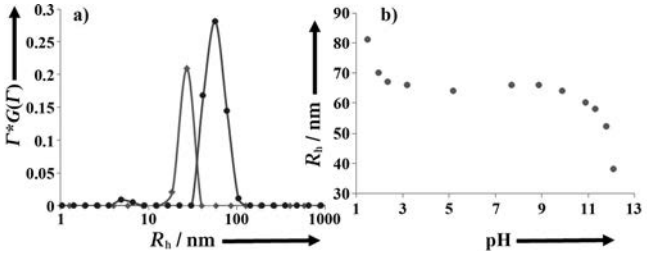

Figure 6. a) DLS results of H·Ds aqueous solution at pH 1.5 (●) and pH 12 (◆) at 90° scattering angle; b) The plot of hydrodynamic radii of vesicles versus pH of the hybrid aqueous solution.

The increase of the pH value leads to further deprotonation of the polar head groups, which consequently increases their net charge. Therefore, the repulsion between the polar heads of the hybrids in the aggregates becomes stronger, resulting in significantly larger curvature of the vesicles, that is, smaller size. The vesicles from the H·Ds hybrids and the "blackberry" structures formed by POM macroions showed the same pH-dependent self-assembly behavior.[22] However, the driving forces for the two aggregates are different. It is the solvophobic interaction that controls the assembly of the H·Ds hybrid surfactant, whilst the counterion-mediated attractive forces and the hydrogen-bonding interactions are the major factors for the "blackberry" formation.

The addition of divalent counterions to an aqueous solution of the H·Ds hybrid caused a decrease in the stability of the self-assembled structures. When 20 μL of 0.02 mg mL^{-1} $CaCl_2$ aqueous solution was added into a 5 mL aqueous solution of the H·Ds hybrid ($\approx$0.2 mg mL^{-1}), the solution became cloudy, and the formation of a large amount of uniform microneedle-like structures was observed. SEM results indicated that the length of the needles is approximately 320 μm, and the diameter of the cross section is approximately 2.7 μm, which is quite similar to the assemblies observed for Anderson-based surfactant on silicon substrate[23] (Figure 7). The microneedle structures showed high contrast

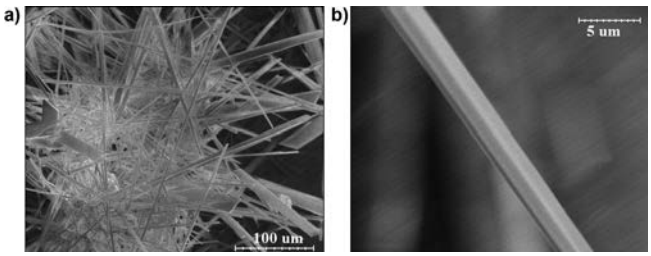

Figure 7. a) SEM image of the microneedle structures. b) Zoom-in image of one needle.

© 2012 Wiley-VCH Verlag GmbH & Co. KGaA, Weinheim

from the iron substrate under SEM mode, suggesting that the polar head groups should be on the surface of the microstructures. Known as the "salting out effect",[24] the addition of Ca^{2+} ions led to stronger interaction among the individual hybrids and their assemblies, which eventually destroyed the vesicles and rearranged the hybrids into highly ordered solid structures with specific orientation.

Conclusion

An organic–inorganic hybrid surfactant with the Dawson-type POM cluster acting as the polar head group has been synthesized; it is able to self-assemble into vesicle structures in polar solvents. The size of the vesicles can be adjusted by hybrid concentration and the solvent polarity. In organic polar solvent, the vesicle formation and their corresponding sizes are dependent on the addition of salts: Zn^{2+} cations can decrease the vesicle size, whilst Na^+ and H^+ cations can screen the repulsive interaction between POM polar head groups and thus increases the size of the vesicles. Due to the positive charge and hydrophobic properties of tetraalkylammonium ions, the addition of these can decrease the surfactant's amphiphilic features and eventually disassemble the vesicle structures. In aqueous solution, raising the solution pH can reversibly decrease the size of the vesicles by shielding the repulsion between polar head groups. The addition of Ca^{2+} triggers the collapse of vesicles into micro-needle structures.

Experimental Section

Sample preparation: Complex $TBA_5H_4[P_2V_3W_{15}O_{62}]$ was synthesized according to the previous literature.[27] The details of the synthesis and characterization of organic ligand L^1 are listed in the Supporting Information. $TBA_5H_4[P_2V_3W_{15}O_{62}]$ (1.0 g, 0.19 mmol) was dissolved in MeCN (30 mL), then L^1 (0.107 g, 0.3 mmol) was added to the solution. The reaction mixture was heated at reflux for 6 days in the dark. The resulting yellow solution was filtered and added dropwise to an excess of diethyl ether with vigorous stirring. The resulting yellow solid was collected and redissolved in minimum volume of MeCN, then reprecipitated by addition of diethyl ether. The yellow precipitate thus obtained was isolated by filtration, dried overnight under vacuum, and recrystallized from acetonitrile by ether diffusion. Yield: 0.90 g (0.16 mmol, 81.4%, based on $TBA_5H_4[P_2V_3W_{15}O_{62}]$). ^{1}H NMR (400 MHz; CD_3CN): $\delta = 6.11$ (s, 1H, NH), 5.72 (s, 6H, $-CH_2-O$), 2.15 (t, 2H, $-CO-CH_2-$), 1.30 (m, 24H, alkyl), 0.917 ppm (t, 3H, CH_3) in addition to the TBA and solvent resonances; FTIR (KBr): $\tilde{\nu} = 3444$ (w), 2960 (m), 2929 (m), 2873 (m), 1483 (m), 1465 (w), 1379, 1083 (s), 1064, 946 (s), 906 (s), 887 (s), 788 (s), 786 (w), 719 cm^{-1}; MS (ESI; CH_3CN): m/z: 2621.7 $[TBA_4Ds]^{2-}$, 1666.7 $[TBA_3Ds]^{3-}$, 1586.5 $[TBA_2HDs]^{3-}$; elemental analysis calcd (%) for $C_{116}H_{254}N_7O_{63}P_2V_3W_{15}$ (5727.64): C 24.32, H 4.47, N 1.71; found: C 25.20, H 4.65, N 1.80.

Static light scattering: A commercial Brookhaven Instrument LLS spectrometer equipped with a solid-state laser operating at $\lambda = 532$ nm was used for measurement of both SLS and DLS. SLS experiments were performed at scattering angles (θ) between 20 and 100°, at 2° intervals. However, due to the large fluctuations in scattered intensities at low scattering angles, we removed the data from 20–40° in the final analysis. Derived from Rayleigh–Gans–Debye equation,[25] partial Zimm plot was used to analyze the SLS data to obtain the radius of gyration (R_g). The partial Zimm plot stems from the following approximate formula: $1/I = C(1+R_g^2 \cdot q^2/3)$, in which R_g is determined from the slope and the intercept of a plot of $1/I$ versus q^2.

Dynamic light scattering: DLS measures the intensity–intensity time correlation function by means of a BI-9000AT multichannel digital correlator. The field correlation function $|g^{(1)}(\tau)|$ was analyzed by the constrained regularized CONTIN method[26] to obtain information on the distribution of the characteristic line width Γ. The normalized distribution function of the characteristic linewidth, $G(\Gamma)$, so obtained, can be used to determine an average apparent translational diffusion coefficient, $D_{app} = \Gamma/q^2$. The hydrodynamic radius R_h is related to D by the Stokes–Einstein equation: $R_h = kT/(6\pi\eta D)$, in which k is the Boltzmann constant, and η is the viscosity of the solvent at temperature T. From DLS measurements, we can obtain the particle-size distribution in solution from a plot of $\Gamma \times G(\Gamma)$ versus R_h. The R_h of the particles is obtained by extrapolating $R_{h,app}$ to zero scattering angle. The normalized distribution function of the characteristic linewidth, $G(\Gamma)$, so obtained, can be used to determine an average apparent translational diffusion coefficient, $D_{app} = \Gamma/q^2$. The hydrodynamic radius R_h is related to D by the Stokes–Einstein equation: $R_h = kT/(6\pi\eta D)$, in which k is the Boltzmann constant, and η is the viscosity of the solvent at temperature T. From DLS measurements, we can obtain the particle-size distribution in solution from a plot of $\Gamma \times G(\Gamma)$ versus R_h. The R_h of the particles is obtained by extrapolating $R_{h,app}$ to zero scattering angle.

Acknowledgements

T.L. acknowledges support from the NSF (CHE1026505), and Sloan Foundation and Lehigh University. L.C. acknowledges support from EPSRC and WestCHEM.

[1] a) C. L. Hill, *Chem. Rev.* **1998**, *98*, 1–2; b) D.-L. Long, R. Tsunashima, L. Cronin, *Angew. Chem.* **2010**, *122*, 1780–1803; *Angew. Chem. Int. Ed.* **2010**, *49*, 1736–1758.
[2] D.-L. Long, L. Cronin, *Chem. Eur. J.* **2006**, *12*, 3698–3706.
[3] D. E. Katsoulis, *Chem. Rev.* **1998**, *98*, 359–388.
[4] a) T. Liu, *Langmuir* **2010**, *26*, 9202–9213; b) T. Liu, E. Diemann, H. L. Li, A. W. M. Dress, A. Müller, *Nature* **2003**, *426*, 59–62; c) P. Yin, D. Li, T. Liu, *Isr. J. Chem.* **2011**, *51*, 191–204; d) G. J. T. Cooper, L. Cronin, *J. Am. Chem. Soc.* **2009**, *131*, 8368–8369; e) C. P. Pradeep, D.-L. Long, L. Cronin, *Dalton Trans.* **2010**, *39*, 9443–9457.
[5] a) C. P. Pradeep, D.-L. Long, G. N. Newton, Y.-F. Song, L. Cronin, *Angew. Chem.* **2008**, *120*, 4460–4463; *Angew. Chem. Int. Ed.* **2008**, *47*, 4388–4391; b) T. Kojima, M. R. Antonio, T. Ozeki, *J. Am. Chem. Soc.* **2011**, *133*, 7248–7251.
[6] S.-T. Zheng, J. Zhang, X.-X. Li, W.-H. Fang, G.-Y. Yang, *J. Am. Chem. Soc.* **2010**, *132*, 15102–15103.
[7] a) J. Zhang, J. Hao, Y. Wei, F. Xiao, P. Yin, L. Wang, *J. Am. Chem. Soc.* **2009**, *131*, 14–15; b) J. Kang, B. Xu, Z. Peng, X. Zhu, Y. Wei, D. R. Powell, *Angew. Chem.* **2005**, *117*, 7062–7065; *Angew. Chem. Int. Ed.* **2005**, *44*, 6902–6905.
[8] a) J. W. Han, C. L. Hill, *J. Am. Chem. Soc.* **2007**, *129*, 15094–15095; b) S.-T. Zheng, J. Zhang, G.-Y. Yang, *Angew. Chem.* **2008**, *120*, 3973–3977; *Angew. Chem. Int. Ed.* **2008**, *47*, 3909–3913.
[9] Y. F. Wang, I. A. Weinstock, *Dalton Trans.* **2010**, *39*, 6143–6152.
[10] a) Y. Yan, L. Wu, *Isr. J. Chem.* **2011**, *51*, 181–190; b) Y. Yan, H. Wang, B. Li, G. Hou, Z. Yin, L. Wu, V. W. W. Yam, *Angew. Chem.* **2010**, *122*, 9419–9422; *Angew. Chem. Int. Ed.* **2010**, *49*, 9233–9236.
[11] a) S. Landsmann, C. Lizandara-Pueyo, S. Polarz, *J. Am. Chem. Soc.* **2010**, *132*, 5315–5321; b) J. J. Giner-Casares, G. Brezesinski, H. Möhwald, S. Landsmann, S. Polarz, *J. Phys. Chem. Lett.* **2012**, *3*, 322–326.
[12] P. Yin, P. Wu, Z. Xiao, D. Li, E. Bitterlich, J. Zhang, P. Cheng, D. V. Vezenov, T. Liu, Y. Wei, *Angew. Chem.* **2011**, *123*, 2569–2573; *Angew. Chem. Int. Ed.* **2011**, *50*, 2521–2525.

 © 2012 Wiley-VCH Verlag GmbH & Co. KGaA, Weinheim

[13] a) J. Zhang, Y.-F. Song, L. Cronin, T. Liu, *J. Am. Chem. Soc.* **2008**, *130*, 14408–14409; b) J. Zhang, Y.-F. Song, L. Cronin, T. Liu, *Chem. Eur. J.* **2010**, *16*, 11320–11324.
[14] Y. Han, Y. Xiao, Z. Zhang, B. Liu, P. Zheng, S. He, W. Wang, *Macromolecules* **2009**, *42*, 6543–6548.
[15] C. P. Pradeep, M. F. Misdrahi, F.-Y. Li, J. Zhang, L. Xu, D.-L. Long, T. Liu, L. Cronin, *Angew. Chem.* **2009**, *121*, 8459–8463; *Angew. Chem. Int. Ed.* **2009**, *48*, 8309–8313.
[16] J. H. Roh, R. Behrouzi, R. M. Briber, L. Guo, D. Thirumalai, S. A. Woodson, *Biophys. J.* **2009**, *96*, 2755.
[17] a) A. Zlotnick, *Virology* **2003**, *315*, 269–274; b) A. Zlotnick, R. Aldrich, J. M. Johnson, P. Ceres, M. J. Young, *Virology* **2000**, *277*, 450–456.
[18] S. L. Heilman-Miller, D. Thirumalai, S. A. Woodson, *J. Mol. Biol.* **2001**, *306*, 1157–1166.
[19] a) J. M. Pigga, M. L. Kistler, C. Y. Shew, M. R. Antonio, T. Liu, *Angew. Chem.* **2009**, *121*, 6660–6664; *Angew. Chem. Int. Ed.* **2009**, *48*, 6538–6542; b) J. M. Pigga, T. Liu, *Inorg. Chim. Acta* **2010**, *363*, 4230–4233; c) J. M. Pigga, J. A. Teprovich, R. A. Flowers, M. R. Antonio, T. Liu, *Langmuir* **2010**, *26*, 9449–9456.
[20] a) D. Bitting, J. H. Harwell, *Langmuir* **1987**, *3*, 500–511; b) G. Silbert, J. Klein, S. Perkin, *Faraday Discuss.* **2010**, *146*, 309–324; c) D. F. Evans, J. B. Evans, R. Sen, G. G. Warr, *J. Phys. Chem.* **1988**, *92*, 784–790; d) J. B. Evans, D. F. Evans, *J. Phys. Chem.* **1987**, *91*, 3828–3829.
[21] a) W.-J. Chen, G.-Z. Li, G.-W. Zhou, L.-M. Zhai, Z.-M. Li, *Chem. Phys. Lett.* **2003**, *374*, 482–486; b) P. Long, A. Song, D. Wang, R. Dong, J. Hao, *J. Phys. Chem. B* **2011**, *115*, 9070–9076; c) J. Du, Y. Tang, A. L. Lewis, S. P. Armes, *J. Am. Chem. Soc.* **2005**, *127*, 17982–17983.
[22] T. Liu, B. Imber, E. Diemann, G. Liu, K. Cokleski, H. L. Li, Z. Q. Chen, A. Muller, *J. Am. Chem. Soc.* **2006**, *128*, 15914–15920.
[23] Y.-F. Song, N. McMillan, D.-L. Long, J. Thiel, Y. Ding, H. Chen, N. Gadegaard, L. Cronin, *Chem. Eur. J.* **2008**, *14*, 2349–2354.
[24] J. O. M. Bockris, H. Egan, *Trans. Faraday Soc.* **1948**, *44*, 151–159.
[25] P. C. Hiemenz, R. Rajagopalan, *Principles of Colloid and Surface Chemistry*, Marcel Dekker, New York, **1997**.
[26] S. W. Provencher, *Comput. Phys. Commun.* **1982**, *27*, 229–242.
[27] R. G. Finke, B. Rapko, R. J. Saxton, P. J. Domaille, *J. Am. Chem. Soc.* **1986**, *108*, 2947–2960.

Received: February 2, 2012
Published online: May 22, 2012

 © 2012 Wiley-VCH Verlag GmbH & Co. KGaA, Weinheim